A&A 478, 121–126 (2008)
DOI: 10.1051/0004-6361:20078618

Astronomy & Astrophysics

The X-ray emission of the most luminous 3CR radio sources

M. Salvati[1], G. Risaliti[1,2], P. Véron[3], and L. Woltjer[1,3]

[1] INAF – Osservatorio Astrofisico di Arcetri, Largo E. Fermi 5, 50125 Firenze, Italy
e-mail: salvati@arcetri.astro.it
[2] Harvard-Smithsonian Center for Astrophysics, 60 Garden Street, Cambridge, MA 02138, USA
e-mail: risaliti@arcetri.astro.it
[3] Observatoire de Haute Provence, CNRS, 04870 St. Michel l'Observatoire, France
e-mail: philippe.veron@oamp.fr

Received 5 September 2007 / Accepted 23 October 2007

ABSTRACT

Context. Although many radio-loud quasars and galaxies have been observed in X-rays, systematic studies of well defined samples are rare.
Aims. We investigate the X-ray properties of the most luminous radio sources in the 3CR catalogue, in order to assess whether they are similar to the most luminous radio-quiet quasars, for instance in the X-ray normalization with respect to the optical luminosity, or in the distribution of the absorption column density.
Methods. We have selected the (optically identified) 3CR radio sources whose 178-MHz monochromatic luminosity lies in the highest factor-of-three bin. The 4 most luminous objects had already been observed in X-rays. Of the remaining 16, we observed 8 randomly chosen ones with XMM-Newton, with the only requirement that half were of type 1 and half of type 2 according to the optical identification.
Results. All targets were detected. The optical-to-X-ray spectral index, α_{ox}, can be computed only for the type 1s and, in agreement with previous studies, is found to be flatter than in radio-quiet quasars of similar luminosity. However, the Compton-thin type 2s have an absorption-corrected X-ray luminosity systematically lower than the type 1s, by a factor which makes them consistent with the radio-quiet α_{ox}. Within the limited statistics, the Compton-thick objects seem to have a reflected component more luminous than the Compton-thin ones.
Conclusions. The extra X-ray component observed in type 1 radio-loud quasars is beamed for intrinsic causes, and is not collimated by the absorbing torus as is the case for the (intrinsically isotropic) disk emission. The extra component can be associated with a relativistic outflow, provided that the flow opening angle and the Doppler beaming factor are $\sim 1/5-1/7$ radians.

Key words. galaxies: active – galaxies: quasars: general – radio continuum: galaxies – X-rays: galaxies

1. Introduction

Strong X-ray emission is a defining property of Active Galactic Nuclei, and radio-loud quasars and galaxies share this property. The most interesting entries in the radio catalogues have been observed repeatedly with all the X-ray satellites launched so far. Although much has been learned, our knowledge is still fragmentary in comparison with the radio-quiet AGN. The latter dominate the X-ray sky, and it is relatively straightforward to assemble large samples which can then be studied at other wavelengths. On the contrary, luminous extragalactic radio sources are rare, and one has to observe them one by one, investing large amounts of satellite time.

There are a few points on which a consensus has been established. The type 1 radio-loud quasars have an X-ray emission stronger than their radio-quiet analogues of similar optical luminosity, which is quantified by a flatter α_{ox} (e.g. Brinkmann et al. 1997, versus Steffen et al. 2006). There are indications that the X-ray photon index Γ is systematically flatter in radio-loud quasars (Shastri et al. 1993; but Brinkmann et al. 1997 have a more cautious view). At any rate, a flatter $\Gamma \sim 1.5-1$ is well established in flat spectrum radio sources and low frequency peaked blazars (Grandi et al. 2006; Fossati et al. 1998). The type 2 radio galaxies are commonly found to host absorbed AGN; a paradigmatic case is the nearby powerful source Cygnus A (Young et al. 2002). Even if absorbed below energies of several keV, the radio galaxies are frequently detected around 1 keV at a level of a few percent of the main emission (Belsole et al. 2006, and references therein). It is unclear whether the residual emission is due to reflection or scattering of the main emission, or is completely unrelated.

The basic picture is the extension of the so-called unified scheme to the case where the accretion disk is complemented by a relativistic outflow ("jet"). The radio galaxies and radio quasars are the misaligned and aligned members, respectively, of the same population. The optical and soft X-ray emission of the former is obscured by some intervening medium, perhaps arranged in a toroidal geometry. The jet emission, because of the Doppler boosting, becomes more and more prominent along a sequence where the line of sight becomes closer to the jet axis, passing from steep spectrum to flat spectrum radio quasars, and to blazars.

In this paper we present and discuss a study of the X-ray properties of the most luminous low frequency radio sources. By selecting at 178 MHz, the frequency of the 3CR catalogue (Bennet 1962), we select sources with a luminous extended, isotropic component, which is thought to arise from the accumulation of relativistic plasma over the entire lifetime of the system. The AGN in our sample are then expected to have had a large *time averaged* power in their past life, whereas the X-ray

Table 1. The sample objects.

Name	Type	Redshift z	Radio luminosity L_r	Magnitude	Exposure time (ks)	References
3C 298	Q	1.439	29.79	16.79 (V)	20 (C)	1
3C 9	Q	2.012	29.72	18.21 (V)	16 (C)	2
3C 257	G	2.474	29.67	18.07 (K)	30 (X)	3
3C 191	Q	1.956	29.55	18.65 (V)	17 (C)	4
3C 239	G	1.781	29.46	22.50 (V)	14 (X)	5
3C 454	Q	1.757	29.39	18.47 (V)	16 (X)	5
3C 432	Q	1.785	29.38	17.96 (V)	11 (X)	5
					20 (C)	4
3C 294	G	1.786	29.35	18.00 (K)	118 (C)	6
3C 249	G	1.554	29.34	18.90 (K)	35 (X)	5
3C 241	G?	1.617	29.30	23.50 (V)	25 (X)	5
3C 318	Q?	1.574	29.30	20.30 (V)	19 (X)	5
3C 205	Q	1.534	29.28	17.62 (V)	5 (X)	5

References. (1) Siemiginowska et al. (2003); (2) Fabian et al. (2003a); (3) Derry et al. (2003); (4) Erlund et al. (2006); (5) our data; (6) Fabian et al. (2003b).

luminosity depends on the *instantaneous* power at the present time. A correlation between the two holds only in a statistical sense. On the other hand, by selecting with respect to an isotropic component we avoid all the uncertainties connected with the Doppler boosting. We restrict ourselves to the 3CR sources at high Galactic latitude ($|b| > 20°$) with optical identification and redshift (Spinrad et al. 1985), and order them with respect to L_r, a radio luminosity parameter equal to the logarithm of the monochromatic luminosity at 178 MHz in W Hz^{-1} m^{-2}. We adopt the concordance cosmology with $\Omega_m = 0.3$, $\Omega_\Lambda = 0.7$, and $H_0 = 70$ km s^{-1} Mpc^{-1}. We neglect the k-correction because all the objects of interest happen to be steep spectrum radio sources, i.e. they have a spectral slope α ($f_\nu \propto \nu^{-\alpha}$) close to 1 in the 100-MHz region. In half a decade, from $L_r = 29.79$ to $L_r = 29.28$, one has 20 objects.

The four most luminous ones had already been observed by previous investigators. We chose at random 8 additional objects among the remaining 16, with the only requirement that 4 were optical type 1 and 4 optical type 2, and observed them with XMM-Newton. One of the 8 (3C 294) had previous Chandra observations, and we did not reobserve it. One further object (3C 432) was also observed with Chandra after our XMM run had been scheduled. Due to the randomness of our choice, we believe that the final sample of 4+8 objects is a fair representation of the highest radio luminosity bin, although a rather slender one. The only infringement to randomness, i.e. the preselection of optical types, implies that we cannot draw inferences about the relative frequency of types from our X-ray data.

2. Observations and data reduction

In Table 1 we report the basic data of the objects in our sample. The columns are: the 3C name; the optical classification, either a type 1 quasar (Q) or a type 2 radio galaxy (G); the redshift z; the radio luminosity parameter L_r; the magnitude in the specified filter; the exposure time t_{exp} in kiloseconds, and the satellite used for the X-ray observation (either X or C for XMM-Newton and Chandra, respectively); and the reference to the X-ray data. The optical data are taken from Spinrad et al. (1985) and from the NASA/IPAC Extragalactic Database (NED); in case of discrepancy, we take the most recent determination; if no data are available in the above catalogues, we resort to the X-ray references listed in the table.

A question mark appended to the optical type indicates an intermediate classification, with characteristic properties of both a quasar and a galaxy present in the same object. In particular, the galaxy 3C 241 has been found to exhibit a broad line in the near-infrared observer-frame spectrum (Hirst et al. 2003), and the broad line object 3C 318 has a very red, underluminous optical continuum (Willott et al. 2000). All the objects in Table 1 are steep spectrum radio sources; this is usually interpreted as evidence of viewing angles substantially larger than the jet beaming.

The data have been processed according to the standard sequence with version 7.0.0 of the XMM SAS package (`http://xmm.esac.esa.int/sas/`). Since we were interested in the nucleus only, we extracted the source events in an aperture of the order of the PSF width (typically three times); the background events were extracted far from possible extended features (jets and lobes); if a diffuse cluster emission was also present, the background extraction region was an annulus immediately exterior to the source.

The analysis software was version 11.3 of XSPEC (`http://heasarc.gsfc.nasa.gov/docs/xanadu/xspec/`). If there were a sufficient number of counts, the spectra were rebinned to a minimum of 15 counts per bin, and analyzed with the χ^2 statistic; otherwise no rebinning was made, and the C statistic was used. The relatively low signal to noise ratio prompted the adoption of very simple spectral models: the most complex combination was

wabs*(powerlaw+zgauss+zwabs*powerlaw)

with the same photon index for the two power laws, and the local absorption fixed at the Galactic value. Quite often even simpler models proved adequate. Our assumption on the photon indices implies the (conservative) assumption that the low energy component is due to hot reflection or to partial covering.

The results are presented in Table 2, which contains the 3C name; the optical and the X-ray type, where the latter is coded U for unabsorbed ($N_H < 10^{22}$ cm^{-2}), A for absorbed (10^{22} cm$^{-2} < N_H < 10^{24}$ cm^{-2}), and T for Compton-thick (10^{24} cm$^{-2} < N_H$); the absorption-corrected luminosity in the rest frame 2−10 keV interval, L_{2-10} (this component cannot be measured in Compton-thick sources); the photon index Γ; the column density N_H intrinsic to the source; the equivalent width EW of an Fe line, computed in the rest frame with respect to

Table 2. Results of the X-ray analysis.

Name	Type	Intrinsic luminosity L_{2-10} (10^{45} erg s^{-1})	Spectral index Γ	Column density $N_{\rm H}$ (10^{22} cm^{-2})	Equivalent width (keV)	Reflected luminosity $L_{\rm refl}$ (10^{44} erg s^{-1})
3C 298	QU	24.7	1.82 (+0.03, −0.03)	0.45 (+0.03, −0.03)	...	...
3C 9	QU	2.92	1.58 (+0.10, −0.10)	...	...	...
3C 257	GA	0.64	1.42 (+0.30, −0.21)	5.5 (+6.4, −2.7)	...	<0.64
3C 191	QU	3.93 (+0.54, −0.09)	1.73 (+0.28, −0.12)	0.38 (+0.26, −0.28)	...	...
3C 239	GT	...	2.10 (+0.65, −0.45)	<0.32	2.5 (+2.5, −1.8)	2.2 (+0.3, −0.3)
3C 454	QU	3.30 (+0.15, −0.15)	1.68 (+0.09, −0.07)	<0.13	<0.17	...
3C 432	QU	2.47 (+0.16, −0.16)	1.91 (+0.20, −0.14)	<0.32	<0.66	...
3C 294	GA	0.80 (+0.16, −0.16)	1.9	84 (+11, −9)	0.20 (+0.13, −0.11)	0.19 (+0.24, −0.08)
3C 249	GT	...	1.76 (+0.32, −0.18)	<0.82	< 0.95	2.3 (+0.4, −0.4)
3C 241	G?A	1.27 (+0.21, −0.17)	1.98 (+0.32, −0.30)	13 (+5, −4)	0.49 (+0.33, −0.31)	1.03 (+0.48, −0.42)
3C 318	Q?U	1.76 (+0.08, −0.08)	1.95 (+0.14, −0.13)	0.29 (+0.17, −0.16)	<0.34	...
3C 205	QU	7.09 (+0.33, −0.33)	2.07 (+0.15, −0.11)	0.43 (+0.18, −0.17)	<0.26	...

the absorption-corrected continuum; the reflected luminosity in the rest frame 2−10 keV interval, $L_{\rm refl}$ (this component cannot be measured if there is a negligible intrinsic $N_{\rm H}$). All errors or upper limits are at the 90% confidence level for one interesting parameter. Sometimes, the data retrieved from the literature are incomplete.

There is a close correspondence between the optical and the X-ray types: all quasars are unabsorbed, while all galaxies (with the possible exception of 3C 249) are absorbed, either Compton-thin or thick. A clearcut Compton-thick example is 3C 239: here only the reflected component is visible, with a spectral index similar to the unabsorbed sources and a very low upper limit on the intrinsic $N_{\rm H}$. The true origin of this component (reflection instead of underluminous unabsorbed emission) is shown by the large equivalent width of the Fe line. The line energy is not compatible with neutral iron [6.67 (+0.17−0.13) keV], suggesting that at least in this case the visible component is indeed reflected from a hot medium which preserves the intrinsic spectral index; the width of the line is very weakly constrained (<0.5 keV).

The X-ray spectrum of 3C 249 is similar to 3C 239, but here the Fe line is not detected. We classify it as a Compton-thick source on the basis of the optical type and the relative weakness of the X-ray emission, however this particular object is compatible with our findings but does not add independent evidence to them. The point representing 3C 249 in Fig. 4 is bracketed in order to signal the uncertain X-ray classification.

Also to be noted is the segregation in X-ray luminosity between type 1s and Compton-thin type 2s: the former are more luminous than 2.5×10^{45} erg s^{-1}, while the latter (after correction for absorption) are less luminous than 8.0×10^{44} erg s^{-1}; the logarithmic mean is 45.70 ± 0.37 and 44.85 ± 0.07, respectively. The two objects with intermediate optical classification, 3C 318 and 3C 241, fall between the two groups, with 45.22 ± 0.03. A consequence of the systematic difference in intrinsic luminosity, which is enhanced by the effects of absorption, is that the Fe line is detected only in type 2 sources. The equivalent widths with respect to the intrinsic continuum are analogous to the radio-quiet AGN (e.g. Bianchi et al. 2007). In all cases (except 3C 239) the line energy is compatible with neutral iron; for consistency, the upper limits on the line EW in type 1s are computed at 6.4 keV.

Figures 1–3 show the X-ray spectra typical of unabsorbed, Compton-thin, and Compton-thick sources (3C 454, 3C 241, and 3C 239, respectively).

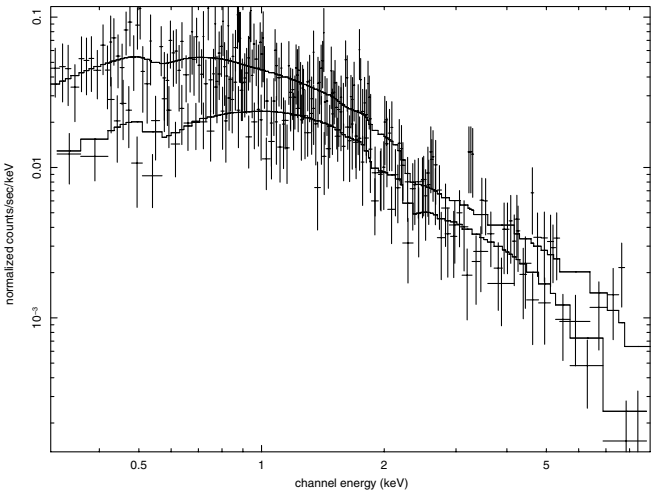

Fig. 1. Data and fitted model for 3C 454. The upper and lower sets refer to PN and MOS, respectively.

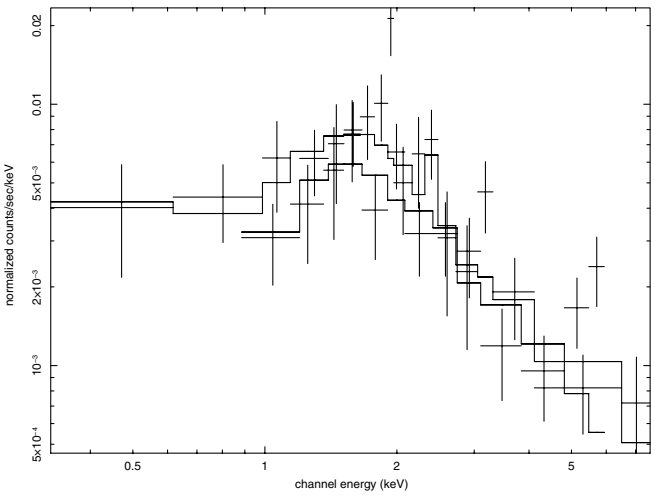

Fig. 2. Same as Fig. 1 for 3C 241.

3. Discussion

The main point of the present work has been noted in the previous section, and is the segregation in intrinsic luminosity between the unabsorbed type 1s and the absorption-corrected, Compton-thin type 2s. This will be shown to have far reaching implications. However our finding is limited by the small

Table 3. The additional sample.

Name	Type	Redshift	Radio luminosity	Intrinsic luminosity	Reflected luminosity	References
		z	L_r	Log(L_{2-10})	Log(L_{refl})	
3C 324	GT	1.206	29.12	...	43.66	1
3C 380	QU	0.691	29.10	45.81	...	2
3C 280	GT	0.997	29.09	...	43.84	3
3C 325	G?A	1.135	29.05	44.85	<43.45	1
3C 309.1	QU	0.904	28.97	45.78	...	2
3C 212	QU	1.049	28.95	45.78	...	4
3C 210	GT	1.169	28.87	...	43.85	1
3C 184	GA	0.994	28.83	44.76	43.14	2
3C 295	GA	0.461	28.82	44.48	42.50	5
3C 265	GA	0.811	28.79	44.70	43.40	6
3C 254	QU	0.734	28.69	45.32	...	2

References. (1) our analysis of Chandra archival data; (2) Belsole et al. (2006); (3) Donahue et al. (2003); (4) Aldcroft et al. (2003); (5) Hardcastle et al. (2006); (6) Bondi et al. (2004).

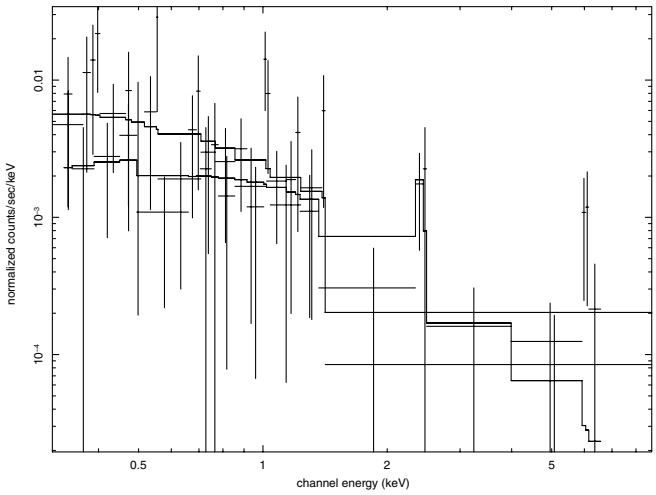

Fig. 3. Same as Fig. 1 for 3C 239.

number of objects involved. In order to increase the statistics, we have collected all the 3CR sources with X-ray observations having optical identification and redshift, high Galactic latitude ($|b| > 20°$), and the radio luminosity parameter L_r in the factor-of-three interval immediately below our fiducial sample, i.e. $28.67 < L_r < 29.28$.

The additional sample contains 46 objects, of which only 12 are observed in X-rays. Relative to the fiducial sample, the additional one is sparsely observed (26% versus 60%); furthermore, we have no control over the criteria by which the observed sources were chosen. In order to confirm or disprove the luminosity segregation which we want to investigate, a crucial point is a possible bias of the additional sample with respect to the orientation of the jet axis. One source is the well known blazar 3C 454.3; its X-ray emission is completely dominated by the jet, so we do not consider it further in the following. The remaining 11 sources have steep radio spectra, and none of them is classified as a blazar; the spectra of three of them (3C 380, 3C 309.1 and 3C 212) become flat above a few GHz, perhaps a hint that their orientation angles are at the lower end of the non-blazar region. Also the distribution of optical properties (4 type 1s, 6 type 2s, and one intermediate type) does not exhibit obvious peculiarities.

Table 3 gives some basic information about the 11 additional sources. We list the 3C name; the optical and X-ray type; the redshift z; the radio luminosity parameter L_r; the intrinsic and reflected X-ray luminosity, L_{2-10} and L_{refl} (actually, the logarithm of the luminosity in erg s^{-1}); and the reference to the X-ray data. 3C 325 is a further case of intermediate optical classification (Grimes et al. 2005).

Figure 4 summarizes the information of Tables 2 and 3: we plot the logarithm of the X-ray luminosity, Log(L_{2-10}) and Log(L_{refl}), against the radio luminosity parameter, L_r. The meaning of the symbols is explained in the caption. For clarity we omit the errorbars: the radio fluxes have typical errors of 1 Jy at the 3C flux limit of 10 Jy, so that the horizontal errorbars are less than 0.04 dex; the X-ray values have typical errors of less than 25%, i.e. less than 0.1 dex. Only the reflected components of Compton-thin galaxies, the empty triangles in the figure, have larger errors of the order of 0.3 dex.

The lower right corner is expected to be underpopulated, given the limit of 10 Jy for the 3C catalogue and a typical depth of 10^{-15} erg cm^{-2} s^{-1} for the X-ray exposures.

The two parallel solid lines sketch the regions occupied by the type 1s and the Compton-thin type 2s, respectively. The difference of about 0.75 dex is fully consistent with the average values found in the previous section for the fiducial sample only, i.e. the addition of more sources confirms the luminosity segregation of the two types. Also, the intermediate optical types are confirmed to lie at intermediate X-ray luminosities. The dotted lines indicate the 5% fraction of the type 1 and type 2 luminosity, respectively. This particular value is generally regarded as an upper limit for the reflected or scattered components, because of various constraints on geometry, efficiency, and optical depth.

In the case of type 1s the optical emission of the AGN is visible, and one can compute the index α_{ox}. We do that for all the type 1s of the fiducial sample; we derive the rest frame monochromatic fluxes at 2 keV and at 2500 Å by means of the observed Γ in the X rays, and by assuming $\alpha = 0.5$ in the optical ($f_\nu \propto \nu^{-\alpha}$). We find $\alpha_{ox} = 1.35 \pm 0.11$. At the average optical flux of our sources, 1.9×10^{31} erg cm^{-2} s^{-1} Hz^{-1}, the radio-quiet AGN have $\alpha_{ox} = 1.65 \pm 0.05$ (Steffen et al. 2006), thus we recover the well-known result (cf. the Introduction) that radio-loud quasars are more X-ray luminous than radio-quiet ones of the same optical luminosity.

This is not true for the radio galaxies, however. If we take into account the lower intrinsic X-ray luminosity of our type 2s we find $\alpha_{ox} \sim 1.64$, fully compatible with the radio-quiet one. Here we do not directly observe the optical emission of the AGN, and we have assumed that type 2s and type 1s with the same L_r have the same intrinsic optical luminosity. The additional component characteristic of the jetted sources becomes visible at

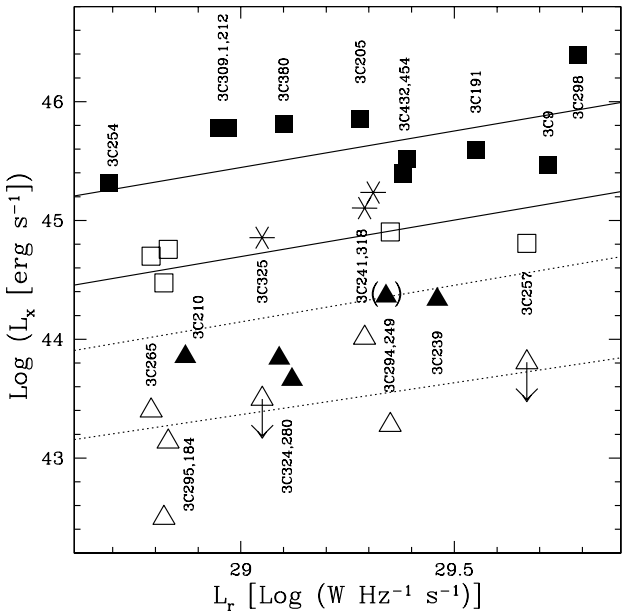

Fig. 4. The X-ray luminosity of the sources in our sample (fiducial plus additional), plotted against the radio luminosity parameter. Filled squares, quasars; stars, intermediate optical types; empty squares, Compton-thin galaxies (the absorption-corrected direct component); filled triangles, Compton-thick galaxies; filled triangle between parentheses, 3C 249 (see text); empty triangles, Compton-thin galaxies (the reflected component). The upper and lower solid lines sketch the regions occupied by type 1s and type 2s, respectively; the dotted lines represent the 5% fraction of the solid lines.

smaller viewing angles for longer wavelengths; indeed, even the high luminosity blazars exhibit optical broad lines with equivalent widths within a factor of two of the non-blazar AGN (Pian et al. 2005; Wills et al. 1995). This points to the jet optical emission never being dominant over the disk optical emission, and gives some ground to our assumption.

The X-ray normalization relative to the optical, and the (meager) evidence provided by the X-ray spectral features (slope Γ, equivalent width of the Fe line), suggest that at the large viewing angles typical of radio galaxies we see only the X-ray emission due to an accretion disk very similar to the radio-quiet AGN. The self-consistent normalization of X-ray, optical and low frequency radio emission does not leave much room for "fossil" quasars, where the extended radio lobes survive for a substantial time after the central engine is switched off.

The additional X-ray emission connected with the "radio loudness" is not seen in radio galaxies, not because of the intervening absorption, but because this emission is intrinsically beamed. The obvious explanation for the beaming is the relativistic aberration of the jet emission. One can try a more quantitative assessment by adopting the distribution of viewing angles proposed by Barthel (1989), according to whom radio-loud AGN appear as type 1s or type 2s if their viewing angle is smaller or larger than ∼44°; thus the average viewing angle is $\theta_1 \sim 31°$ and $\theta_2 \sim 69°$ for the two classes, respectively. Within the type 1 class, one finds the blazar subclass which corresponds to viewing angles smaller than the jet beaming angle, $\theta_b < 10°$.

If one chooses the most favorable scenario, i.e. a jet of constant length and a very flat spectral slope ($\Gamma = 1$), the ratio of the brightness in the two directions θ_b and θ_1 is

$$R_X = [(1 - \beta\cos\theta_1)/(1 - \beta\cos\theta_b)]^2, \qquad \beta = \sqrt{1 - \gamma^{-2}}$$

where γ is the bulk Lorentz factor of the jet. This ratio is equal to about 80 for $\gamma = 15$, as suggested by the analysis of the wide band spectral energy distribution of blazars (Ghisellini et al. 1998). Indeed, by using the maximum viewing angle for a blazar, θ_b, instead of the average one, we have further underestimated R_X. We conclude that the typical X-ray luminosity of high L_r blazars should be R_X times the typical X-ray luminosity of steep spectrum quasars of comparable L_r, i.e. at least 3×10^{47} erg s^{-1}. No such blazar is known. A possible solution to this inconsistency could be a geometrically wide, stratified jet: here the narrow and fast spine would be responsible for the blazar properties, while the slower (but still relativistic) sheath would produce the wide angle additional component. Similar schemes have been suggested both for AGN (Chiaberge et al. 2000) and for Gamma Ray Bursts (Eichler & Levinson 2003).

The above equation for R_X can in principle be applied to the two directions θ_1 and θ_2 to derive the residual jet emission in radio galaxies. This however has nothing to do with the L_{refl} points in Fig. 4: they refer to a spectral component produced above the absorbing material, at a distance of ∼parsecs from the source, whereas time variability constrains the blazar emission to much smaller dimensions (e.g. Ghisellini et al. 1998).

The correct comparison for the L_{refl} points is with the 5-percent-fraction dotted lines. In Fig. 4 the empty triangles lie around or below the lower dotted line, which implies that the reflected component of Compton-thin type 2s has the expected normalization with respect to the intrinsic disk component. The filled triangles, instead, are systematically higher, and lie around or below the higher dotted line, as if they were normalized to the wide jet component. In other words, if one insisted on attributing the visible emission of Compton-thick objects to reprocessing of the disk emission only, one would have to accept reprocessed fractions as high as 30%.

The statistics is certainly not compelling, however a possible scenario is one where the optical depth at large viewing angles is not the same in all objects. Compton-thin and Compton-thick type 2 objects would be viewed at similar angles, around 70°, and would have relatively little and relatively large amounts of matter around them, respectively. Thus the Compton thickness would be related to a larger covered solid angle, perhaps so large as to reprocess also the moderately beamed wide jet emission. Under this hypothesis the peculiar position of 3C 241 is accounted for. This source exhibits at the same time an intermediate X-ray luminosity and a relatively large N_H, as if the line of sight were grazing at the same time the boundaries of the wide jet and the boundaries of a particularly large absorber: indeed, here the reprocessing fraction is as high as 8%, and the corresponding empty triangle falls in the region of Compton-thick sources.

4. Summary

We have studied the X-ray properties of a sample representative of the most luminous 3CR sources. There is a clear difference in absorption-corrected X-ray luminosity between the type 1s and the type 2s in our sample, with the latter being a factor of about 6 less luminous than the former. The difference does not change if we augment our sample with similar objects retrieved from the literature.

While the optical-to-X-ray slope α_{ox} of the type 1s is flatter, the type 2s have the same α_{ox} of the radio-quiet AGN of similar power.

We argue that, at least at high radio luminosities, the quasi-isotropic, disk-produced X-ray emission is at the same level as in radio-quiet AGN, and that the additional emission related to the

"radio loudness" is anisotropic for intrinsic reasons, independent of the circumnuclear absorption. The anisotropy is likely due to Doppler beaming, however there are arguments which disfavor a single zone narrow jet with a Lorentz factor ~15: perhaps these values apply only to the spine of the jet, with a wider and slower sheath being responsible for the additional emission of type 1s.

We find marginal evidence that Compton-thick sources have larger amounts of absorbing matter around them, which extends so close to the axis of the system as to be able to reprocess the emission of the wide jet as well as the disk.

References

Aldcroft, T. L., Siemiginowska, A., Elvis, M., et al. 2003, ApJ, 597, 751
Barthel, P. D. 1989, ApJ, 336, 606
Belsole, E., Worrall, D. M., & Hardcastle, M. J. 2006, MNRAS, 366, 339
Bennet, A. S. 1962, MemRAS, 68, 163
Bianchi, S., Guainazzi, M., Matt, G., & Fonseca Bonilla, N. 2007 [arXiv:astro-ph/0703433]
Bondi, M., Brunetti, G., Comastri, A., & Setti, G. 2004, MNRAS, 354, L43
Brinkmann, W., Yuan, W., & Siebert, J. 1997, A&A, 319, 413
Chiaberge, M., Celotti, A., Capetti, A., & Ghisellini, G. 2000, A&A, 358, 104
Derry, P. M., O'Brien, P. T., Reeves, J. N., et al. 2003, MNRAS, 342, L53
Donahue, M., Daly, R. A., & Horner, D. J. 2003, ApJ, 584, 643
Eichler, D., & Levinson, A. 2003, ApJ, 596, L14
Erlund, M. C., Fabian, A. C., Blundell, K. M., Celotti, A., & Crawford, C. S. 2006, MNRAS, 371, 29
Fabian, A. C., Celotti, A., & Johnstone, R. M. 2003a, MNRAS, 338, L7
Fabian, A. C., Sanders, J. S., Crawford, C. S., & Ettori, S. 2003b, MNRAS, 341, 729
Fossati, G., Maraschi, L., Celotti, A., Comastri, A., & Ghisellini, G. 1996, MNRAS, 299, 433
Ghisellini, G., Celotti, A., Fossati, G., Maraschi, L., & Comastri, A. 1998, MNRAS, 301, 451
Grandi, P., Malaguti, G., & Fiocchi, M. 2006, ApJ, 642, 113
Grimes, J. A., Rawlings, S., & Willott, C. J. 2005, MNRAS, 359, 1345
Hardcastle, M. J., Evans, D. A., & Croston, J. H. 2006, MNRAS, 370, 1893
Hirst, P., Jackson, N., & Rawlings, S. 2003, MNRAS, 346, 1009
Pian, E., Falomo, R., & Treves, A. 2005, MNRAS, 361, 919
Shastri, P., Wilkes, B. J., Elvis, M., & McDowell, J. 1993, ApJ, 410, 29
Siemiginowska, A., Aldcroft, T. L., Bechtold, J., et al. 2003, PASA, 20, 113
Spinrad, H., Djorgovski, S., Marr, J., & Aguilar, L. 1985, PASP, 97, 932
Steffen, A. T., Strateva, I., Brandt, W. N., et al. 2006, AJ, 131, 2826
Young, A. J., Wilson, A. S., Terashima, Y., Arnaud, K. A., & Smith, D. A. 2002, ApJ, 564, 176
Willott, C. J., Rawlings, S., & Jarvis, M. J. 2000, MNRAS, 313, 237
Wills, B. J., Thompson, K. L., Han, M., et al. 1995, ApJ, 447, 139